J|A|C|S
ARTICLES
Published on Web 08/01/2006

Triphenylene Analogues with $B_2N_2C_2$ Cores: Synthesis, Structure, Redox Behavior, and Photophysical Properties

Cory A. Jaska, David J. H. Emslie,‡ Michael J. D. Bosdet, Warren E. Piers,* Ted S. Sorensen, and Masood Parvez

Contribution from the Department of Chemistry, University of Calgary, 2500 University Drive North West, Calgary, Alberta, Canada T2N 1N4

Received May 19, 2006; E-mail: wpiers@ucalgary.ca

Abstract: A series of alkyl (**1**−**3**), aryl (**6**), and benzo-annulated (**4**, **5**) heteroaromatic triphenylene analogues with $B_2N_2C_2$ cores have been synthesized via chelation of pyridazine derivatives using difunctional Lewis acidic diborabiphenyl precursors. In contrast to triphenylene, NICS(1) calculations on **1** suggested high aromaticities for the central (−11.3 ppm) and outer borabenzene rings (−7.7 ppm), along with nonaromatic behavior for the pyridazine ring (−0.7 ppm). Crystal structure analyses supported this analysis. When the *a*- and *c*-faces of the pyridazine moiety were free of substitution (**1**, **3**), planar structures resulted, but upon substitution, a twisted $B_2N_2C_2$ core was observed due to steric repulsion of neighboring hydrogen atoms (e.g., **5**). The increase of steric bulk from H (**1**) to ^{i}Pr (**3**) in the planar species was found to result in a dimeric, head-to-tail herringbone packing motif, held together by close intermolecular B···N interactions of 3.39 Å. One-electron reduction by Cp^*_2Co was found to afford the radical anions of **3** and **5**, which were characterized by broad, featureless singlets in the EPR spectra; $[\mathbf{3}]^{\bullet-}[Cp^*_2Co]^+$ was characterized by X-ray crystallography. While the planar structures (**1**−**4**) were observed to possess weak fluorescence (Φ_F = 0.02−0.08) with either yellow−orange (ca. 555 nm) or green emission (521 nm), the twisted structures (**5**, **6**) were found to be nonfluorescent.

Introduction

Polycyclic aromatic hydrocarbons (PAHs) have been enjoying a renewed interest due to their potential application in organic-based optical and electronic devices that are expected to be key components in the next generation of lightweight, flexible, and inexpensive molecular electronics.[1] For example, triphenylenes have been used as planar mesogenic cores in columnar discotic liquid crystals due to their self-assembly behavior via $\pi-\pi$ interactions,[2] which have found application in organic light-emitting diodes (OLEDs),[3] solar cells,[4] and organic field-effect transistors (OFETs) as a result of their high charge carrier mobilities.[5] While an all-carbon triphenylene core can provide an electron-rich, *p*-type (donor) semiconducting material, the use of heteroaromatic cores based on hexaazatriphenylene can provide access to electron-poor, *n*-type (acceptor) materials.[6] In addition, recent interest in boron-containing π-conjugated systems has led to the development of new types of optoelectronic materials[7] that have found application as colorimetric chemosensors.[8] Thus, the replacement of C−C units in PAH structures by isoelectronic boron−nitrogen moieties might significantly alter the electronic characteristics of these compounds while maintaining the existing structural features, resulting in new and desirable chemical and physical properties (e.g., emission color) that may be beneficial in the development of new classes of hybrid organic/inorganic-based materials.

One potential synthetic route toward boron- and nitrogen-containing PAH structures could involve the integration of neutral borabenzene or anionic boratabenzene rings[9] into

‡ Present address: Department of Chemistry, McMaster University, 1280 Main Street W. Hamilton, Ontario, Canada L8S 4M1.

(1) (a) Mullen, K.; Rabe, J. P. *Ann. NY Acad. Sci.* **1998**, *852*, 205. (b) Watson, M. D.; Fechtenkotter, A.; Mullen, K. *Chem. Rev.* **2001**, *101*, 1267. (c) Bendikov, M.; Wudl, F.; Perepichka, D. F. *Chem. Rev.* **2004**, *104*, 4891.
(2) (a) McKenna, M. D.; Barbera, J.; Marcos, M.; Serrano, J. L. *J. Am. Chem. Soc.* **2005**, *127*, 619. (b) Ikeda, M.; Takeuchi, M.; Shinkai, S. *Chem. Commun.* **2003**, 1354. (c) Barbera, J.; Garces, A. C.; Jayaraman, N.; Omenat, A.; Serrano, J. L.; Stoddart, J. F. *Adv. Mater.* **2001**, *13*, 175. (d) Paraschiv, I.; Giesbers, M.; van Lagen, B.; Grozema, F. C.; Abellon, R. D.; Siebbeles, L. D. A.; Marcelis, A. T. M.; Zuilhof, H.; Sudholter, E. J. R. *Chem. Mater.* **2006**, *18*, 968.
(3) (a) Freudenmann, R.; Behnisch, B.; Hanack, M. *J. Mater. Chem.* **2001**, *11*, 1618. (b) Seguy, I.; Jolinat, P.; Destruel, P.; Farenc, J.; Mamy, R.; Bock, H.; Ip, J.; Nguyen, T. P. *J. Appl. Phys.* **2001**, *89*, 5442.
(4) (a) Kumar, S. *Curr. Sci.* **2002**, *82*, 256. (b) Oukachmih, M.; Destruel, P.; Seguy, I.; Ablart, G.; Jolinat, P.; Archambeau, S.; Mabiala, M.; Fouet, S.; Bock, H. *Sol. Energy Mater. Sol. Cells* **2005**, *85*, 535.
(5) (a) Adam, D.; Closs, F.; Frey, T.; Funhoff, D.; Haarer, D.; Ringsdorf, H.; Schuhmacher, P.; Siemensmeyer, K. *Phys. Rev. Lett.* **1993**, *70*, 457. (b) Adam, D.; Schuhmacher, P.; Simmerer, J.; Haussling, L.; Siemensmeyer, K.; Etzbachi, K. H.; Ringsdorf, H.; Haarer, D. *Nature* **1994**, *371*, 141.
(6) (a) Pieterse, K.; van Hal, P. A.; Kleppinger, R.; Vekemans, J. A. J. M.; Janssen, R. A. J.; Meijer, E. W. *Chem. Mater.* **2001**, *13*, 2675. (b) Gearba, R. I.; Lehmann, M.; Levin, J.; Ivanov, D. A.; Koch, M. H. J.; Barbera, J.; Debije, M. G.; Piris, J.; Geerts, Y. H. *Adv. Mater.* **2003**, *15*, 1614. (c) Crispin, X.; Cornil, J.; Friedlein, R.; Okudaira, K. K.; Lemaur, V.; Crispin, A.; Kestemont, G.; Lehmann, M.; Fahlman, M.; Lazzaroni, R.; Geerts, Y.; Wendin, G.; Ueno, N.; Bredas, J. L.; Salaneck, W. R. *J. Am. Chem. Soc.* **2004**, *126*, 11889. (d) Chang, T. H.; Wu, B. R.; Chiang, M. Y.; Liao, S. C.; Ong, C. W.; Hsu, H. F.; Lin, S. Y. *Org. Lett.* **2005**, *7*, 4075.
(7) (a) Yamaguchi, S.; Akiyama, S.; Tamao, K. *J. Am. Chem. Soc.* **2000**, *122*, 6335. (b) Yamaguchi, S.; Shirasaka, T.; Tamao, K. *Org. Lett.* **2000**, *2*, 4129. (c) Yamaguchi, S.; Shirasaka, T.; Akiyama, S.; Tamao, K. *J. Am. Chem. Soc.* **2002**, *124*, 8816. (d) Wakamiya, A.; Ide, T.; Yamaguchi, S. *J. Am. Chem. Soc.* **2005**, *127*, 14859.
(8) (a) Yamaguchi, S.; Akiyama, S.; Tamao, K. *J. Am. Chem. Soc.* **2001**, *123*, 11372. (b) Kubo, Y.; Yamamoto, M.; Ikeda, M.; Takeuchi, M.; Shinkai, S.; Yamaguchi, S.; Tamao, K. *Angew. Chem., Int. Ed.* **2003**, *42*, 2036.

hydrocarbon-based aromatic structures. However, few examples of B_nN_n analogues of PAH frameworks exist. Pioneering work by Dewar et al. in the late 1950s led to the synthesis of diazadibora analogues of pyrene and anthracene,[10] along with azabora analogues of naphthalene[11] and phenanthrene,[12] in which the isoelectronic BN moieties replaced peripheral C−C positions. A decade later, the preparation of the 9-borataanthracene anion was accomplished by the groups of Bickelhaupt[13] and Jutzi,[14] while more recently, all three possible isomers of boratanaphthalene have been introduced.[15] Despite these successes, little research has focused on internalizing the boron and nitrogen atoms in PAH analogues (e.g., using B and N as annulation points at the junction of two rings), which might provide additional chemical stability to the resulting materials. Two exceptions to this were provided by Dewar et al., in which BN moieties were internalized into the central ring of two triphenylene analogues to afford BNC_4 and B_3N_3 (borazine) cores surrounded by a conjugated carbon periphery,[16,17] and Ashe et al., where the two annulation points of naphthalene were replaced by a BN moiety.[18] In addition, select borabenzene derivatives have been demonstrated to possess nonlinear optical (NLO) responses[19] and strong fluorescence,[20] but these properties have not been systematically investigated in the heteroatom-containing PAH analogues reported thus far.

Our group has recently published a synthetic route to 2,2′-diborabiphenyls, a family of versatile Lewis acidic chelators that provide access to $B_2N_2C_2$ PAH analogues when reacted with appropriate difunctional bases.[21] In this paper, we report our investigations on the synthesis and structural characterization of a series of alkyl, aryl, and benzo-annulated $B_2N_2C_2$ triphenylene analogues. The redox chemistry of these derivatives was examined, along with an evaluation of the aromaticity of these novel compounds by nucleus-independent chemical shift (NICS) calculations and an investigation of their fluorescent properties. These studies reveal a striking difference between these compounds and their all-carbon PAH analogues.

Scheme 1

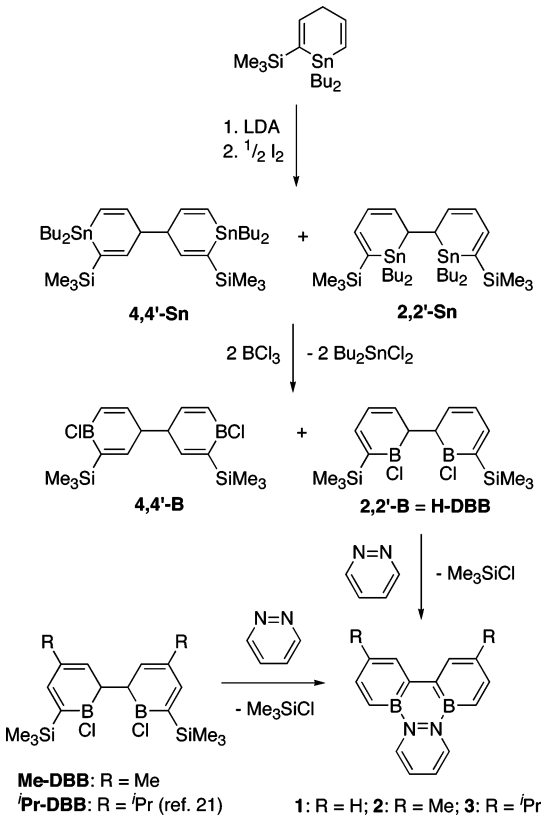

Results and Discussion

Synthesis of $B_2N_2C_2$-Substituted Triphenylene Analogues. Our initial report described a synthetic route to a diborabiphenyl precursor that incorporated an *iso*-propyl group in the 4-position relative to boron on each ring (*i*Pr-DBB in Scheme 1); an analogous sequence can be employed to gain the related methyl-substituted derivative **Me-DBB**. While substitution in this position was deemed essential to direct the regiochemistry of the C−C coupling of the 2,2′-diborabiphenyl framework, it was also desirable to access the unsubstituted species **H-DBB**, which was accomplished as shown in Scheme 1. Deprotonation of the stannacyclohexadiene with LDA, followed by coupling with 0.5 equiv of I_2, afforded a mixture of **2**,**2′-Sn** and **4**,**4′-Sn** in a ratio of ca. 60:40. This (likely kinetic) ratio was essentially invariant over a range of conditions. Transmetalation with BCl_3 afforded the desired **H-DBB** (or **2**,**2′-B**) as the major product (60%), along with the isomeric **4**,**4′-B** as an inseparable, air- and moisture-sensitive mixture. The reaction of **H-DBB** with the bidentate Lewis base pyridazine was found to afford the dark red **1**,[22] an isoelectronic analogue of triphenylene in which the inner C_6 core has been replaced with a $B_2N_2C_2$ ring (Scheme 1). These reactions proceed rapidly with loss of Me_3SiCl after an allowed suprafacial 1,5-hydrogen shift. Unfortunately, only moderate isolated yields of **1** were obtained (41%) along with a large amount of insoluble cross-linked material, likely due to the presence of the linear species **4**,**4′-B**. The methyl- and *iso*-propyl-substituted analogues **2** and **3** were similarly prepared from the corresponding **Me-DBB** and ***i*Pr-DBB** boracycles (Scheme 1). The reactions of ***i*Pr-DBB** with a variety of

(9) (a) Fu, G. C. *Adv. Organomet. Chem.* **2001**, *47*, 101. (b) Herberich, G. E.; Ohst, H. *Adv. Organomet. Chem.* **1986**, *25*, 199.
(10) Chissick, S. S.; Dewar, M. J. S.; Maitlis, P. M. *Tetrahedron Lett.* **1960**, *1* (44), 8.
(11) (a) Dewar, M. J. S.; Dietz, R. *J. Chem. Soc.* **1959**, 2728. A more recent paper has reinvestigated this work; see: (b) Paetzold, P.; Stanescu, C.; Stubenrauch, J. R.; Bienmuller, M.; Englert, U. *Z. Anorg. Allg. Chem.* **2004**, *630*, 2632.
(12) Dewar, M. J. S.; Kubba, V. P.; Pettit, R. *J. Chem. Soc.* **1958**, 3073.
(13) (a) Van Veen, R.; Bickelhaupt, F. *J. Organomet. Chem.* **1971**, *30*, C51. (b) Van Veen, R.; Bickelhaupt, F. *J. Organomet. Chem.* **1974**, *77*, 153.
(14) Jutzi, P. *Angew. Chem., Int. Ed. Engl.* **1972**, *11*, 53.
(15) (a) Boese, R.; Finke, N.; Henkelmann, J.; Maier, G.; Paetzold, P.; Reisenauer, H. P.; Schmid, G. *Chem. Ber.* **1985**, *118*, 1644. (b) Ashe, A. J., III; Al-Ahmad, S.; Kampf, J. W.; Young, V. G., Jr. *Angew. Chem., Int. Ed. Engl.* **1997**, *36*, 2014. (c) Ashe, A. J., III; Fang, X.; Kampf, J. W. *Organometallics* **1999**, *18*, 466. (d) Herberich, G. E.; Cura, E.; Ni, J. *Inorg. Chem. Commun.* **1999**, *2*, 503.
(16) Culling, G. C.; Dewar, M. J. S.; Marr, P. A. *J. Am. Chem. Soc.* **1964**, *86*, 1125.
(17) However, these compounds were poorly characterized by present day standards, relying primarily on elemental analysis and molecular weight determinations for structural elucidation, with no further investigations into their resulting optical or electronic properties.
(18) Fang, X.; Yang, H.; Kampf, J. W.; Banaszak Holl, M. M.; Ashe, A. J., III. *Organometallics* **2006**, *25*, 513.
(19) (a) Hagenau, U.; Heck, J.; Hendrickx, E.; Persoons, A.; Schuld, T.; Wong, H. *Inorg. Chem.* **1996**, *35*, 7863. (b) Behrens, U.; Meyer-Friedrichsen, T.; Heck, J. *Z. Anorg. Allg. Chem.* **2003**, *629*, 1421.
(20) (a) Lee, B. Y.; Wang, S.; Putzer, M.; Bartholomew, G. P.; Bu, X.; Bazan, G. C. *J. Am. Chem. Soc.* **2000**, *122*, 3969. (b) Lee, B. Y.; Bazan, G. C. *J. Am. Chem. Soc.* **2000**, *122*, 8577.
(21) (a) Emslie, D. J. H.; Piers, W. E.; Parvez, M. *Angew. Chem., Int. Ed.* **2003**, *42*, 1252. (b) Ghesner, I.; Piers, W. E.; Parvez, M.; McDonald, R. *Organometallics* **2004**, *23*, 3085.

(22) IUPAC name: bisborino[1,2-*c*:2′,1′-*e*]pyridazino[1,2-*a*][1,2,3,6]-diazadiborine.

Scheme 2

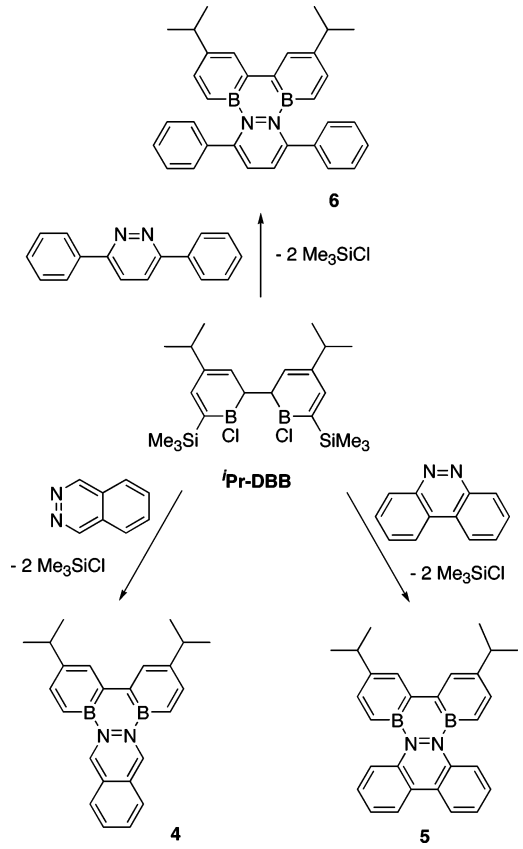

difunctional Lewis bases, such as phthalazine, benzo[*c*]cinnoline, or diphenylpyridazine, were found to afford the substituted $B_2N_2C_2$ triphenylene analogues of benzo[*b*]triphenylene (**4**), dibenzo[*a*,*c*]triphenylene (**5**), and 1,4-diphenyltriphenylene (**6**) (Scheme 2).

Compounds **1**−**6** were found to be moderately air- and moisture-stable, soluble in nonpolar solvents, such as hexanes, and able to endure column chromatography using dry neutral alumina under argon. Good thermal stabilities were also found, as **1** could be vacuum sublimed at 80 °C without decomposition, while the thermogravimetric analyses (TGA) of **3**−**6** showed onset decomposition temperatures of 128−150 °C with $T_{5\%}$ values (temperature at which 5% mass loss was observed) in the range of 160−250 °C.

NICS Calculations on 1: As there are three distinctly different heterocycles that comprise **1**, their individual aromaticities were evaluated by computational methods for a direct comparison to triphenylene. Among the many different methods used to calculate and quantify aromaticity based on magnetic properties, nucleus-independent chemical shift (NICS) calculations have emerged recently as an easily computed, generally applicable criterion to evaluate the aromaticity/antiaromaticity/nonaromaticity character of planar π-conjugated organic ring systems.[23,24] Thus, the calculated NICS(1) values at the B3LYP/6-31G* level for **1** were found to be −7.7 ppm for the outer C_5B borabenzene rings, −11.3 ppm for the central $B_2N_2C_2$ ring, and −0.7 ppm for the outer C_4N_2 pyridazine ring (Figure 1, Table S1 in Supporting Information).

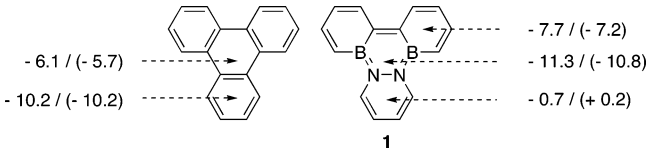

Figure 1. NICS(1) values for triphenylene and **1** at the B3LYP/6-31G* level (values in parentheses are at the B3LYP/6-311+G** level). See Table S1 in the Supporting Information.

These values suggest that the middle ring is aromatic (cf. benzene = −11.2 ppm),[25] while the outer borabenzene rings have a slightly reduced aromatic character, and the pyridazine ring is distinctly nonaromatic in nature. This is the opposite trend to that observed for triphenylene, in which the outer rings were found to be more aromatic (−10.2 ppm) than the central ring (−6.1 ppm). Similar values for both species were found using the B3LYP/6-311+G** basis set. These opposing aromaticity trends for triphenylene and **1** are completely consistent with the analysis of their structural properties (vide supra), which indicate inverse bonding behavior for their central rings. These trends are reproduced closely in the computed structures (Table S2). The middle $B_2N_2C_2$ ring in **1** also displayed a greatly enhanced aromaticity when compared to that of other BN heterocyclic species, such as borazine $[HB-NH]_3$, which has a calculated NICS(0.5) value of −3.2 ppm.[26] Furthermore, the structural data associated with a 1,2-diaza-3,6-diborin monocyclic compound with the $C_2B_2N_2$ core reported by Siebert and Huttner et al. some years ago[27] suggest localized multiple bonding and low aromaticity in this related system. In **1**, the greater degree of aromaticity in the central ring may be a result of enhanced participation of the nitrogen lone pairs toward B=N double bonding; the nitrogen lone pairs in borazine have been found to remain more localized on the nitrogen atoms and thus do not contribute to any significant ring current.[28] Although the relative aromaticity of the isomers of $(CH)_2B_2N_2$ as measured by NICS methodology was found to vary significantly with the positioning of the atoms in the ring,[29] it is curious that the central ring in **1** acquires aromaticity, particularly at the expense of the pyridazine ring,[30] and represents a notable difference in behavior of **1** versus triphenylene.[31]

Structural Analysis of $B_2N_2C_2$-Substituted Triphenylene Analogues: The molecular structures of **1**, **3**, and **5** were

(23) (a) Schleyer, P. v. R.; Maerker, C.; Dransfeld, A.; Jiao, H.; Hommes, N. J. R. v. E. *J. Am. Chem. Soc.* **1996**, *118*, 6317. (b) Chen, Z.; Wannere, C. S.; Corminboeuf, C.; Puchta, R.; Schleyer, P. v. R. *Chem. Rev.* **2005**, *105*, 3842.

(24) The NICS method is a measure of the abnormal proton chemical shift of aromatic molecules by the induced ring current that is due to cyclic σ or π electron delocalization, and whose values can either be negative (suggestive of diatropic ring currents and aromaticity) or positive (suggestive of paratropic ring currents and antiaromaticity). The standard method for NICS calculations is NICS(1), which is calculated at a distance of 1 Å above the plane of the ring in order to minimize the influence from the σ framework while maximizing the contributions from the π system.

(25) Moran, D.; Stahl, F.; Bettinger, H. F.; Schaefer, H. F., III; Schleyer, P. v. R. *J. Am. Chem. Soc.* **2003**, *125*, 6746.

(26) Schleyer, P. v. R.; Jiao, H.; Hommes, N. J. R. v. E.; Malkin, V. G.; Malkina, O. L. *J. Am. Chem. Soc.* **1997**, *119*, 12669.

(27) Siebert, W.; Full, R.; Schmidt, H.; von Seyerl, J.; Halstenberg, M.; Huttner, G. *J. Organomet. Chem.* **1980**, *191*, 15.

(28) (a) Fowler, P. W.; Steiner, E. *J. Phys. Chem. A* **1997**, *101*, 1409. (b) Soncini, A.; Domene, C.; Engelberts, J. J.; Fowler, P. W.; Rassat, A.; van Lenthe, J. H.; Havenith, R. W. A.; Jenneskens, L. W. *Chem.−Eur. J.* **2005**, *11*, 1257.

(29) Cernusak, I.; Fowler, P. W.; Steiner, E. *Mol. Phys.* **2000**, *98*, 945.

(30) A NICS(1) value of −12.50 ppm was reported recently for pyridazine: Fabian, J.; Lewars, E. *Can. J. Chem.* **2004**, *82*, 50.

(31) An analogous series of NICS calculations were performed on the less planar B_2N_2 analogue of benzo[*c*]cinnoline (Table S3). The high deviation from planarity of the central $B_2N_2C_2$ and N_2C_4 rings precluded meaningful NICS values for these rings, but the outer BC_5 rings were found to be slightly less aromatic than those in **1** (NICS(1) = −4.53 ppm), probably due to the less planar configuration of these rings in comparison to those in **1**. The outer C_6 rings of **5** had NICS values similar to those of benzene (−10.33 ppm), indicating a high degree of aromaticity in these rings.

Table 1. Selected Bond Lengths and Torsion Angles for **1**, **3**, **5**, [**3**]$^{\bullet-}$[Cp*$_2$Co]$^+$, and [**5**]$^{\bullet-}$[Cp*$_2$Co]$^+$

	1	**3**	**5**	[**3**]$^{\bullet-}$[Cp*$_2$Co]$^+$	[**5**]$^{\bullet-}$[Cp*$_2$Co]$^+$
			Bond Lengths (Å)		
B(1)−N(1)	1.464(4)	1.455(2)	1.439(2)	1.486(6)	1.466(4)
B(2)−N(2)	1.455(5)	1.460(2)	1.436(2)	1.481(5)	1.482(4)
N(1)−N(2)	1.422(4)	1.410(2)	1.414(2)	1.431(4)	1.430(3)
B(1)−C(5)	1.514(6)	1.528(2)	1.525(3)	1.512(6)	1.519(5)
C(5)−C(6)	1.373(5)	1.357(2)	1.354(3)	1.369(6)	1.378(4)
C(6)−C(7)	1.432(5)	1.440(2)	1.448(2)	1.402(6)	1.422(4)
C(7)−C(8)	1.369(5)	1.365(2)	1.359(2)	1.398(5)	1.379(4)
C(8)−C(9)	1.438(4)	1.433(2)	1.440(2)	1.410(5)	1.420(4)
B(1)−C(9)	1.517(5)	1.517(2)	1.537(3)	1.510(6)	1.527(5)
C(9)−C(10)	1.422(5)	1.413(2)	1.401(2)	1.458(5)	1.444(4)
B(2)−C(10)	1.514(5)	1.528(2)	1.543(3)	1.503(6)	1.511(5)
C(10)−C(11)	1.435(5)	1.438(2)	1.439(2)	1.403(5)	1.425(4)
C(11)−C(12)	1.369(5)	1.365(2)	1.364(2)	1.389(5)	1.381(4)
C(12)−C(13)	1.416(5)	1.437(2)	1.450(2)	1.413(5)	1.408(4)
C(13)−C(14)	1.376(5)	1.364(2)	1.355(2)	1.375(5)	1.375(4)
B(2)−C(14)	1.513(5)	1.528(2)	1.530(3)	1.514(5)	1.513(5)
N(1)−C(1)	1.399(4)	1.399(2)	1.425(2)	1.383(5)	1.413(4)
C(1)−C(2)	1.345(5)	1.336(2)	1.399(2)	1.341(6)	1.405(4)
C(2)−C(3)	1.433(6)	1.416(2)	1.460(3)	1.435(6)	1.460(4)
C(3)−C(4)	1.335(5)	1.343(2)	1.406(2)	1.337(6)	1.412(4)
N(2)−C(4)	1.409(4)	1.392(2)	1.429(2)	1.377(5)	1.402(4)
C(1)−C(15)			1.394(3)		1.393(4)
C(15)−C(16)			1.384(2)		1.386(4)
C(16)−C(17)			1.384(3)		1.379(4)
C(17)−C(18)			1.379(3)		1.375(4)
C(2)−C(18)			1.402(2)		1.402(4)
C(3)−C(19)			1.400(3)		1.397(4)
C(19)−C(20)			1.383(3)		1.379(4)
C(20)−C(21)			1.383(3)		1.384(4)
C(21)−C(22)			1.378(2)		1.392(4)
C(4)−C(22)			1.395(2)		1.397(4)
H(C5)−H(C15)			2.252		2.247
H(C14)−H(C22)			2.190		2.258
			Torsion Angles (deg)		
B(1)−N(1)−N(2)−B(2)	1.3(4)	−0.7(2)	25.3(2)	−0.1(4)	−29.5(4)
B(1)−C(9)−C(10)−B(2)	−0.4(4)	0.3(2)	15.9(2)	−0.1(5)	−19.3(4)
N(1)−N(2)−B(2)−C(10)	−2.7(4)	4.3(2)	−14.5(2)	−2.7(5)	19.7(4)
N(2)−B(2)−C(10)−C(9)	2.2(4)	−4.1(2)	−6.4(2)	2.8(5)	5.1(4)
C(10)−C(9)−B(1)−N(1)	−1.1(4)	3.4(2)	−5.7(2)	−2.7(5)	10.0(4)
C(9)−B(1)−N(1)−N(2)	0.6(4)	−3.2(2)	−15.3(2)	2.8(5)	14.9(4)

confirmed by X-ray crystallography (Figures 2a, 3a, and 4a, respectively). Compounds **1** and **3** were found to adopt a planar, fused ring system (Figures 2b and 3b) analogous to that found in triphenylene.[32] In accord with the NICS calculations, the C═C double bonds in the outer three rings for both **1** and **3** were found to be partially localized with alternating longer (average 1.43 Å) and shorter (average 1.36 Å) bond lengths. The "long" C−C bonds are still shorter than the expected value for a typical C(sp^2)−C(sp^2) single bond (e.g., 1.493 Å in biphenyl),[33] which suggests some degree of delocalization. The central $B_2N_2C_2$ rings of both **1** and **3** were found to contain approximately the same bond lengths: B−N 1.46 Å (average), B−C 1.52 Å (average), N−N 1.42 Å, and C−C 1.42 Å (Table 1). These distances suggest dominance of the resonance form **1B** over **1A** (Scheme 3), as the B−N and C−C bond lengths were more indicative of double bonds (e.g., shorter than that found in the nonchelate compound borabenzenepyridine: 1.558(3) Å[15a]), while the B−C and N−N bond lengths were more indicative of single bonds (e.g., B−C in borabenzenepyridine 1.465(4) and 1.482(4)[15a] Å; N−N in free pyridazine 1.346 Å).[34] These structural parameters are in contrast to those found in triphenylene, in which the three outer rings contain delocalized C═C double bonds (average 1.398 Å) connected by three C(sp^2)−C(sp^2) single bonds (average 1.471 Å).[32]

Scheme 3

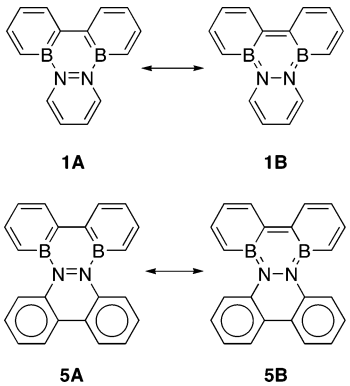

The packing of **1** (Figure 2c) showed the familiar herringbone motif, where the closest intermolecular B···N distance between the molecules in parallel columns was 3.67 Å, with an angle of 66.4° between the molecules in the columns and the closest carbon edge-to-π face distance of 3.70 Å between molecules in adjacent columns. This packing motif is structurally analogous to that found in triphenylene, which also displays herringbone

(32) Collings, J. C.; Roscoe, K. P.; Thomas, R. L.; Batsonov, A. S.; Stimson, L. M.; Howard, J. A. K.; Marder, T. B. *New J. Chem.* **2001**, *25*, 1410.
(33) Charbonneau, G. P.; Delugeard, Y. *Acta Crystallogr. B* **1977**, *33*, 1586.
(34) Blake, A. J.; Rankin, D. W. H. *Acta Crystallogr. C* **1991**, *47*, 1933.

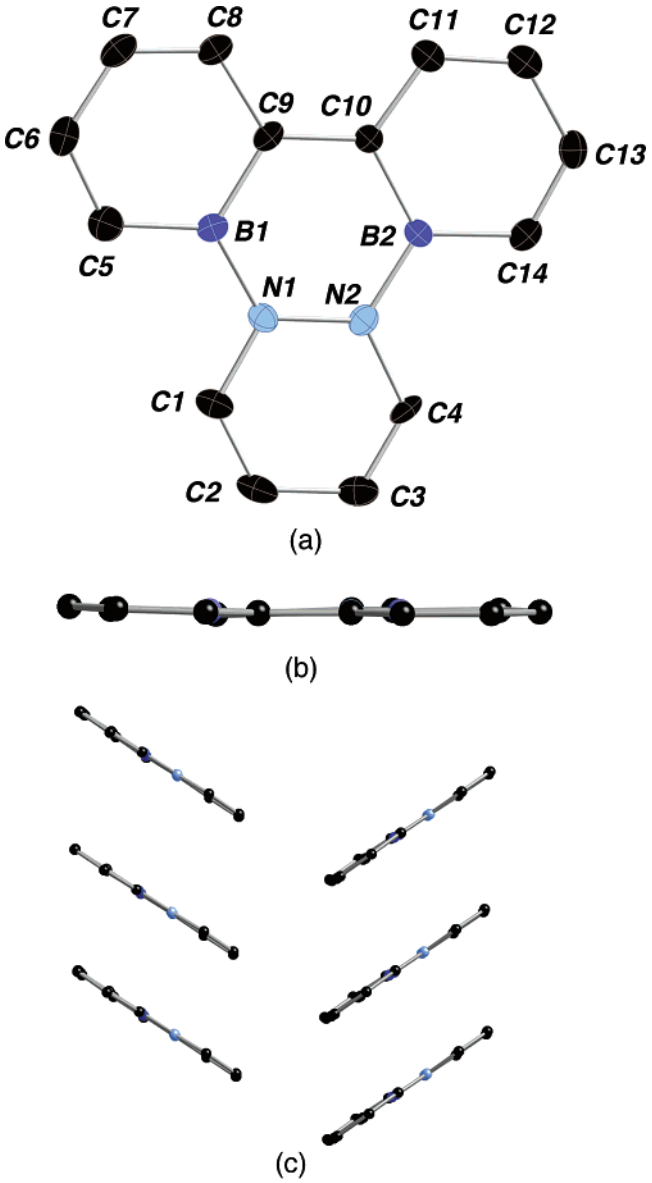

Figure 2. (a) Molecular structure of **1** (thermal ellipsoids, 50%). All hydrogen atoms have been omitted for clarity. (b) Side view of **1**. (c) Herringbone packing motif of **1**. See Table 1 for a list of bond lengths and torsion angles.

packing with distances of ca. 3.3 Å between the parallel molecules, an angle of 63.2° between the columns, and a distance of 3.59 Å for the closest edge-to-face interaction.[32] In contrast, the packing of **3** (Figure 3c) adopts a dimeric herringbone motif, which contains two close intermolecular B···N distances of 3.39 and 3.53 Å (Figure 3d), with an angle of 73.1° between the columns and a distance of 3.59 Å for the closest edge-to-face interaction.

In the case of compound **5**, a nonplanar, twisted geometry was observed due to steric repulsion of the 3,3′-hydrogen atoms of the diborabiphenyl moiety and the opposing 3,3′-hydrogen atoms of the benzo[*c*]cinnoline moiety (Figure 4a), characterized by short intramolecular H···H distances of 2.190 and 2.252 Å. As a result, the central $B_2N_2C_2$ ring was found to contain large torsion angles (e.g., B−N−N−B 25.3(2)°, B−C−C−B 15.9(2)°) compared to the torsion angles found in the planar **1** (1.3(4) and −0.4(4)°, respectively) and **3** (−0.7(2) and 0.3(2)°, respectively). Again, alternating "long" and "short" C−C bonds were observed for the outer two diborabiphenyl rings (average 1.44 and 1.36 Å, respectively), whereas the outer two annulated benzene rings of the benzo[*c*]cinnoline moiety were found to contain delocalized C═C double bonds (average 1.39 Å). While the central $B_2N_2C_2$ ring was found to contain slightly shorter B−N and C−C bonds (1.44 (average) and 1.40 Å, respectively) and slightly longer B−C bonds (average 1.54 Å) than those found in **3** (cf. B−N 1.46 Å, C−C 1.42 Å, B−C 1.52 Å), the N−C bonds were found to lengthen to 1.43 Å (cf. 1.40 Å in **3**), which is more suggestive of resonance form **5B** (Scheme 3). Due to the significant twist in the central core in **5** (Figure 4b), no close π-stacking, herringbone, or intermolecular B···N interactions were observed in the packing diagram.

Cyclic Voltammetry of $B_2N_2C_2$-Substituted Triphenylene Analogues: Cyclic voltammetry experiments on **1** in THF were found to result in two reversible reduction waves at $E_{1/2} = -1.16$ and − 1.85 V (vs SCE), which correspond to the formation of a stable radical anion and a dianion species, respectively (Table 2; see Figure S1 in the Supporting Information for a representative example). An irreversible oxidation wave was observed at 0.56 V, which indicates that the formation of a stable radical cation is not likely. A minor shift toward a more negative first reduction potential was observed from **1**−**3** (**1**, −1.16 V; **2**, −1.21 V; **3**, −1.24 V), with no significant effect on the second reduction potential (**1** and **3**, −1.85 V; **2**, −1.89 V). For the ^{i}Pr series **3**−**6**, the more rigidly planar species **3** and **4** (−1.32 V) were found to be more difficult to reduce than **5** (−1.03 V) and **6** (−1.20 V), which possess a more twisted, less aromatic core resulting from steric interactions between neighboring protons (vide infra). In comparison, triphenylene has been observed to have reversible reduction waves at −2.42 and −2.97 V[35] and reversible oxidation waves at 1.73 and 2.49 V[36] (both vs Ag/AgCl). Thus, the $B_2N_2C_2$ analogues are significantly more susceptible to reduction than the all carbon derivatives.

Table 2. Cyclic Voltammetry Data for **1**−**6**[a]

	THF		CH_2Cl_2	
	reduction (V)	oxidation (V)	reduction (V)	oxidation (V)
1	−1.85 (r)	+0.56 (i)	−2.14 (i)	+0.60 (i)
	−1.16 (r)		−1.35 (r)	
2	−1.89 (r)	+0.69 (i)	−1.25 (r)	+0.76 (i)
	−1.21 (r)			
3	−1.85 (r)	+0.65 (i)	−2.02 (i)	+0.81 (i)
	−1.24 (r)		−1.28 (r)	
4	−1.32 (r)		−1.34 (r)	+1.16 (i)
5	−1.45 (r)		−1.44 (r)	+1.32 (i)
	−1.03 (r)		−1.01 (r)	
6	−1.68 (r)		−1.80 (i)	+0.78 (i)
	−1.20 (r)		−1.21 (r)	
triphenylene	−2.42 (r)[b]	+1.73 (r)[c]		
	−2.97 (r)	+2.49 (r)		

[a] Cyclic voltammetry was performed at a Pt electrode in 1×10^{-3} M solutions with 0.1 M [^{n}Bu$_4$N][PF$_6$] as the supporting electrolyte at a scan rate of 200 mV/s. All $E_{1/2}$ values were referenced internally to Cp_2Fe and are reported relative to saturated calomel electrode (SCE): r = reversible, i = irreversible. [b] Performed in liquid Me_2NH at ca. −50 °C with [^{n}Bu$_4$N]Br as the supporting electrolyte. See ref 35. [c] Performed in liquid SO_2 at −50 °C with [^{n}Bu$_4$N][PF$_6$] as the supporting electrolyte. See ref 36.

Radical Anions and Dianions of $B_2N_2C_2$-Substituted Triphenylene Analogues: The above electrochemical data suggest that compounds **1**−**6** should undergo more facile

(35) Meerholz, K.; Heinze, J. *J. Am. Chem. Soc.* **1989**, *111*, 2325.
(36) Dietrich, M.; Heinze, J. *J. Am. Chem. Soc.* **1990**, *112*, 5142.

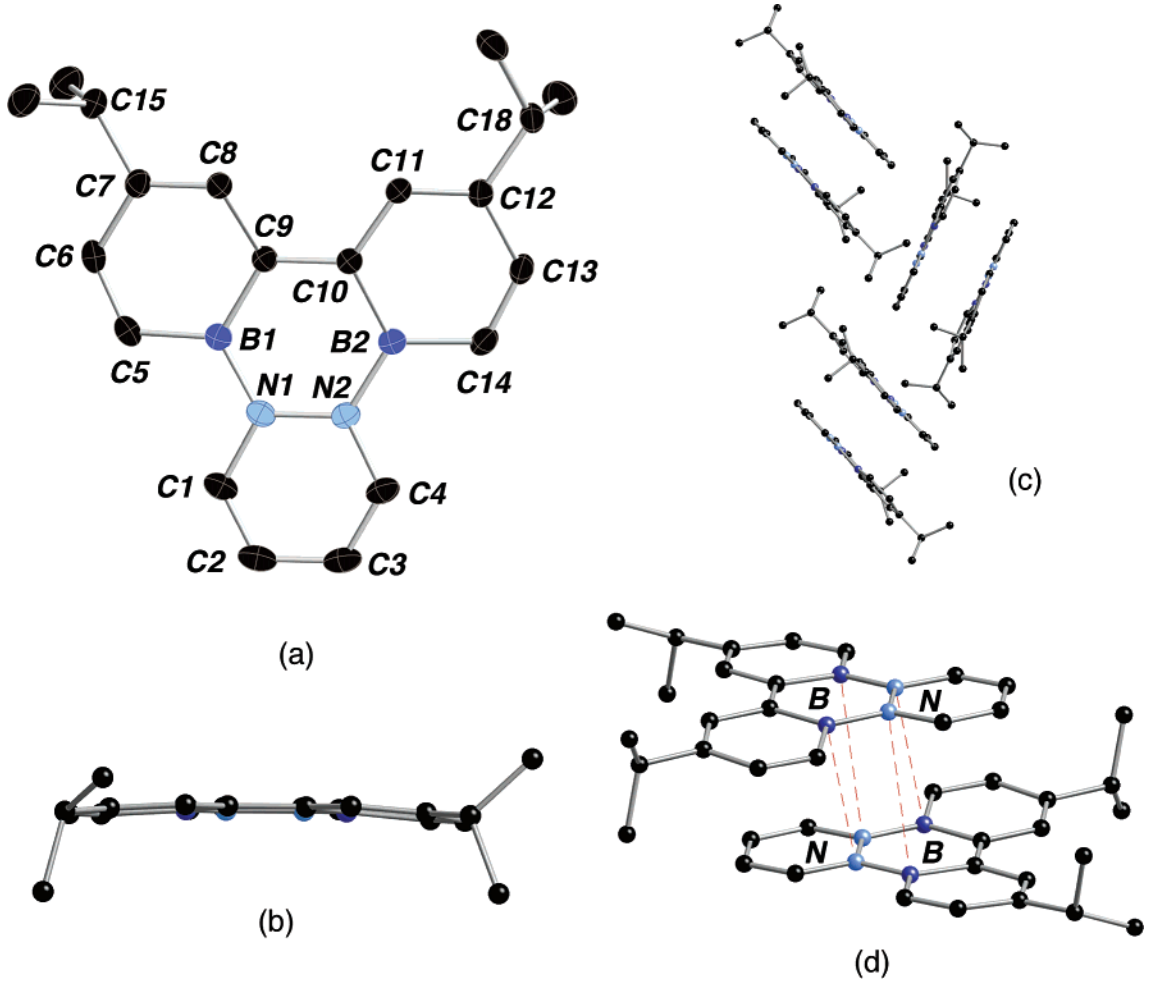

Figure 3. (a) Molecular structure of **3** (thermal ellipsoids, 50%). All hydrogen atoms have been omitted for clarity. (b) Side view of **3**. (c) Dimeric herringbone packing motif of **3**. (d) Head-to-tail dimers of **3**. See Table 1 for a list of bond lengths and torsion angles.

chemical reduction than triphenylene, which usually requires powerful reductants, such as the alkali metals.[37] Thus, the chemical reduction of **3** or **5**[21a] with the relatively mild reductant Cp_2*Co was found to result in the selective formation of the radical anions [**3**]$^{\bullet-}$[Cp*$_2$Co]$^+$ (Scheme 4) or [**5**]$^{\bullet-}$[Cp*$_2$Co]$^+$.[21a] The ^{1}H NMR spectrum of a purple solution of [**3**]$^{\bullet-}$[Cp*$_2$Co]$^+$ showed only a broad signal due to the Cp* methyl groups at 2.72 ppm, while the EPR spectrum displayed a broad, featureless singlet with $g_{iso} = 2.002$ (Figure S2, Supporting Information). This spectrum was acquired at 25 °C; lowering the temperature did not improve the resolution of the signal; similar spectral characteristics were observed for [**5**]$^{\bullet-}$[Cp*$_2$Co]$^+$. The featureless EPR resonances may be a reflection of small heteroatom hyperfine splittings due to the substantial π-component within the B═N linkages, which are not resolved in the spectra acquired.[38]

The structures of [**3**]$^{\bullet-}$[Cp*$_2$Co]$^+$ and [**5**]$^{\bullet-}$[Cp*$_2$Co]$^+$ were also verified by X-ray crystallography; the molecular structure and packing diagram for [**3**]$^{\bullet-}$[Cp*$_2$Co]$^+$ are shown in Figure 5, while the packing diagram for [**5**]$^{\bullet-}$[Cp*$_2$Co]$^+$ is depicted in Figure 6. Relevant metrical data are given in Table 1. When compared to their neutral counterparts, both [**3**]$^{\bullet-}$ and [**5**]$^{\bullet-}$ displayed a lengthening of the C−C, B−N, and N−N bonds in the central $B_2N_2C_2$ cores, in addition to a moderate equalization of the alternating long and short C−C bonds in the outer two borabenzene rings. These bond length changes were expected, as the SOMO of [**1**]$^{\bullet-}$ (Figure S3, Supporting Information) contains a nodal plane along the molecule's C_2 axis as well as two nodes within both of the borabenzene rings, which leads to more antibonding behavior and thus longer bond lengths. The packing of [**3**]$^{\bullet-}$[Cp*$_2$Co]$^+$ displayed columns of π-stacked anions and cations, with distances between the planar [**3**]$^{\bullet-}$ and the nearest Cp* ring on the order of 3.5 Å. Conversely, the packing of [**5**]$^{\bullet-}$[Cp*$_2$Co]$^+$ showed no π-stacking interactions between anion and cation due to the nonplanar nature of [**5**]$^{\bullet-}$ (Figure 6).

To access the dianion of **3**, a more powerful reductant in Li metal was required. Thus, the reaction of **3** in THF-d_8 over a Li mirror in the presence of 12-crown-4 (12-c-4) was found to result in the formation of a purple solution after 3 days at 25 °C. The EPR spectrum displayed a broad, featureless singlet due to the formation of the intermediate radical anion [**3**]$^{\bullet-}$[Li(12-c-4)]$^+$ (Scheme 4), which was further confirmed by the observation of only broad signals in the ^{1}H NMR spectrum. After a further 3 days at 25 °C, formation of a dark red solution

(37) (a) Lemaire, O.; De Backer, M.; Devos, A.; Sauvage, F. X. *Synth. Met.* **2001**, *123*, 61. (b) Jones, M. T.; Ahmed, R. H. *J. Phys. Chem.* **1980**, *84*, 2913. (c) Arick, M. R.; van Broekhoven, J. A. M.; Pijpers, F. W.; de Boer, E. *J. Am. Chem. Soc.* **1972**, *94*, 7531. (d) de Boer, E.; Grotens, A. M.; Smid, J. *J. Am. Chem. Soc.* **1970**, *92*, 4742.
(38) Lichtblau, A.; Kaim, W.; Schulz, A.; Stahl, T. *J. Chem. Soc., Perkin Trans. 2* **1992**, 1497.

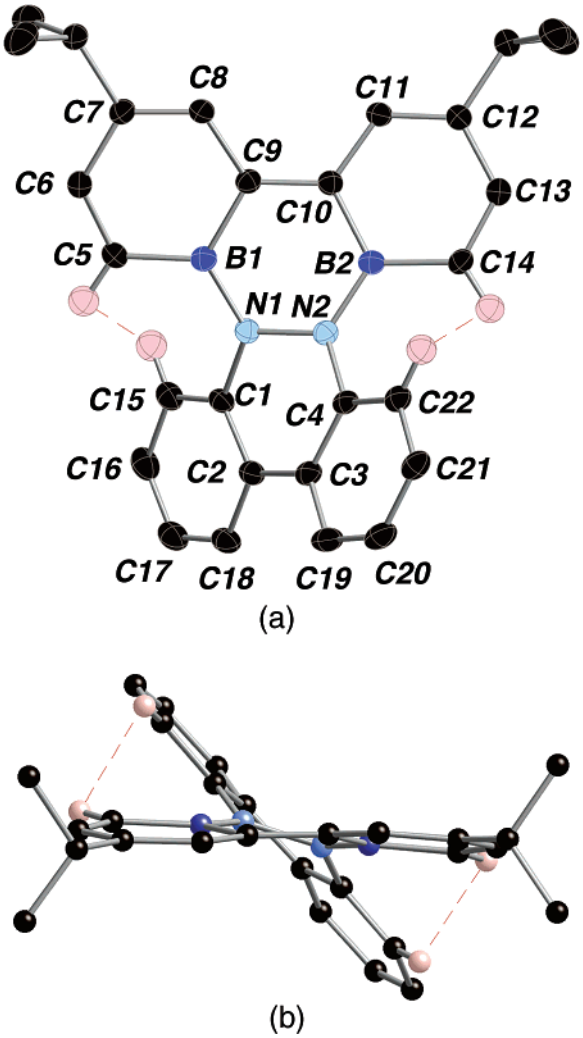

Figure 4. (a) Molecular structure of **5** (thermal ellipsoids, 50%). All hydrogen atoms have been omitted for clarity, except those attached to C5, C14, C15, and C22. (b) Side view of **5**. See Table 1 for a list of bond lengths and torsion angles.

Scheme 4

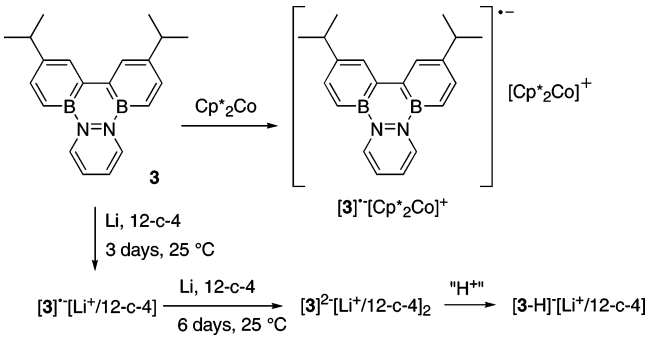

was observed. The ^{1}H NMR spectrum at 0 °C indicated the presence of an unsymmetrical species that can be attributed to the dianion $[\mathbf{3}]^{2-}[\mathrm{Li(12\text{-}c\text{-}4)}]_2^+$, as well as a second unsymmetrical species that has been tentatively assigned as the diamagnetic monoanionic species $[\mathbf{3}\text{-H}]^-[\mathrm{Li(12\text{-}c\text{-}4)}]^+$, resulting from protonation of the dianion $[\mathbf{3}]^{2-}[\mathrm{Li(12\text{-}c\text{-}4)}]_2^+$ (Scheme 4). Upon warming the sample to 25 °C, only the signals associated with $[\mathbf{3}\text{-H}]^-[\mathrm{Li(12\text{-}c\text{-}4)}]^+$ remained distinguishable, while those associated with $[\mathbf{3}]^{2-}[\mathrm{Li(12\text{-}c\text{-}4)}]_2^+$ were broadened and lost in the baseline. It is likely that the formation of the

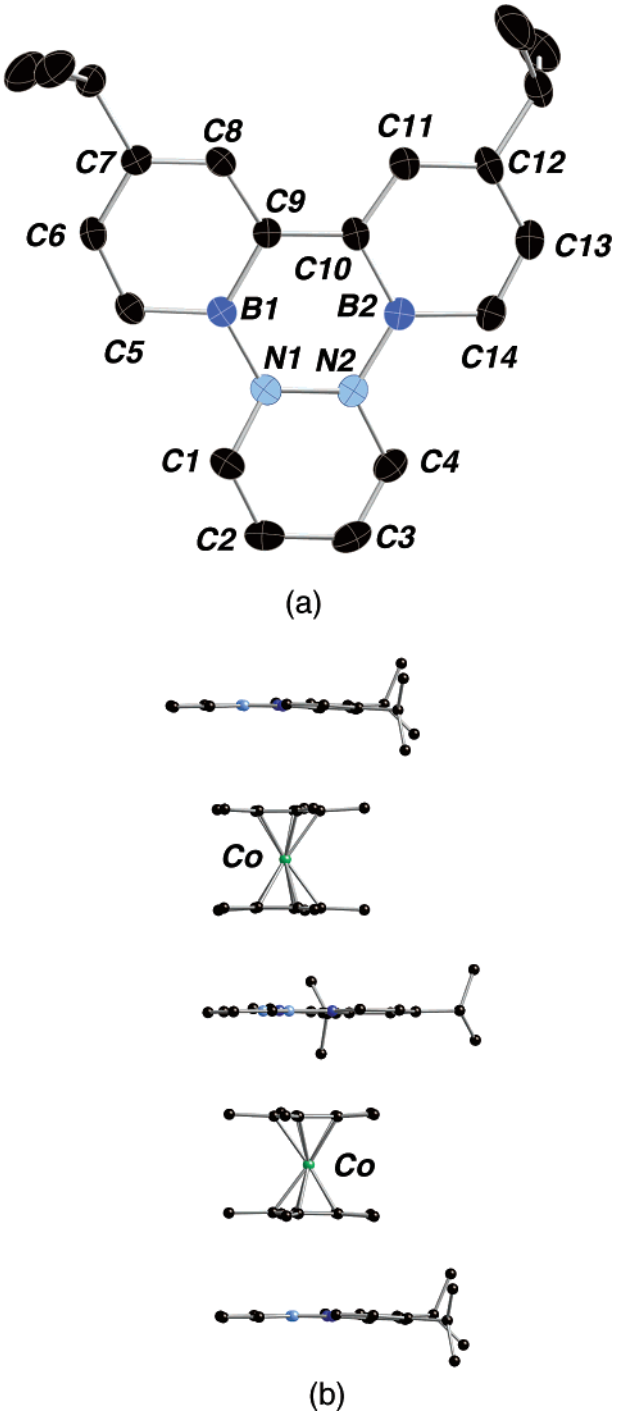

Figure 5. (a) Molecular structure of $[\mathbf{3}]^{\bullet-}$ (thermal ellipsoids, 50%). All hydrogen atoms have been omitted for clarity. (b) Packing diagram of $[\mathbf{3}]^{\bullet-}[\mathrm{Cp^*_2Co}]^+$ showing π-stacking between the anions and cations. See Table 1 for a list of bond lengths and torsion angles.

diamagnetic monoanionic $[\mathbf{3}\text{-H}]^-$ resulted from the reaction of the dianion $[\mathbf{3}]^{2-}$ with protic impurities in the solvent, as has been previously observed in the case of pyrene dianions,[39] or via deprotonation of the solvent itself. The sensitive nature of this dianion $[\mathbf{3}]^{2-}$ has so far precluded isolation of suitable single crystals, but the unsymmetrical nature of the molecule as indicated by ^{1}H NMR spectroscopy most likely indicates Li^+ coordination at different rings. Investigations on the dianion and its protonated derivative are continuing.

(39) Schnieders, C.; Mullen, K.; Huber, W. *Tetrahedron* **1984**, *40*, 1701.

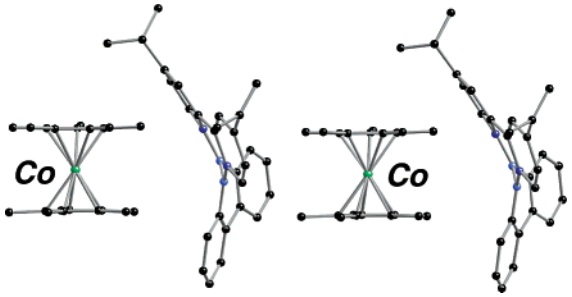

Figure 6. Packing diagram of $[\mathbf{5}]^{\bullet-}[Cp^*_2Co]^+$. The molecular structure of this compound was reported in ref 21a. See Table 1 for a list of bond lengths and torsion angles.

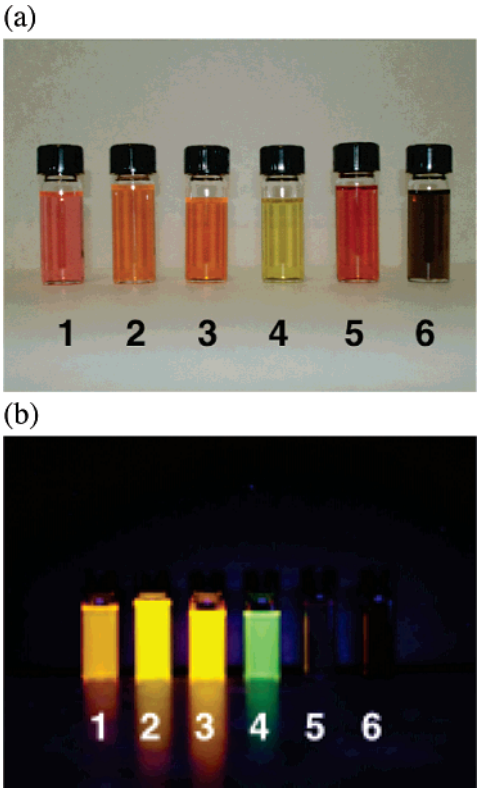

Figure 7. (a) Cyclohexane solutions of **1**−**6**. (b) Fluorescence of **1**−**6** after irradiation at 365 nm.

UV−Visible and Fluorescence Spectroscopy of $B_2N_2C_2$-Substituted Triphenylene Analogues: The triphenylene derivatives **1**−**3** all form highly colored red−orange solutions (Figure 7a) and display strong charge-transfer absorptions in the visible region of their UV−visible spectra (Figure 8; Table 3). For example, absorptions at $\lambda_{max} = 546$ nm for **1** (Figure 8), 536 nm for **2**, and 536 nm for **3** were observed in the UV−vis spectra of hexanes solutions, along with some partially resolved vibrational fine structure. These absorptions presumably arise through charge transfer of an electron from the HOMO, which is located primarily on the central $B_2N_2C_2$ ring, to the LUMO, which is located on the two C_5B borabenzene rings (Figure S4, Supporting Information). In contrast to **1**, the HOMOs of the unsubstituted analogues of **4** and **5** were found to be located more predominantly on the phthalazine (Figure S5, Supporting Information) and benzo[*c*]cinnoline (Figure S6, Supporting Information) moieties, while the LUMOs remained largely unaltered. These charge-transfer bands were red-shifted to $\lambda_{max} = 557$ nm for **1**, 546 nm for **2**, and 545 nm for **3** when acquired in CH_2Cl_2, due to stronger solvent interactions with the π-electrons that lower the energy of the excited state.[40] Similarly, CH_2Cl_2 solutions of **4**, **5**, and **6** also displayed strong charge-transfer absorptions at $\lambda_{max} = 447$, 501, and 622 nm, respectively. While the absorption maximum in **6** was found to be red-shifted by 77 nm from that of **3**, due to exocyclic conjugation effects from the two phenyl groups,[40a] the absorption maxima in **4** and **5** were found to be blue-shifted by 98 and 44 nm, respectively. This is in contrast to the all-carbon analogues benzo[*b*]triphenylene and dibenzo[*a*,*c*]triphenylene, in which the presence of one and two additional annulated benzene rings results in successive red-shifted α, β, and γ bands due to an increase in the conjugation length.[41] Thus, this anomalous blue shift may be, in part, due to diminished conjugation resulting from the presence of two isolated chromophores in the form of diborabiphenyl and phthalazine/benzo[*c*]cinnoline frameworks, which may be caused by a nonplanar geometry resulting from either steric interactions (in the case of **5**) or decreased rigidity (in the case of **4**). In comparison, solutions of triphenylene are colorless with only $\pi-\pi^*$ transitions observed in the UV ($\lambda_{max} = 318$ and 273 nm) and no charge-transfer absorptions in the visible.

Excitation of dilute cyclohexane solutions of **1**−**3** at 260 nm was found to result in yellow−orange fluorescence (Figure 7b) with an emission peak centered around $\lambda_{max} = 551-558$ nm, along with the mirror symmetrical vibrational fine structure at longer wavelengths (583−586 nm) (Figure 8, Table 3). Upon increasing the concentration of **1** from 10^{-5} to 10^{-3} M, a new featureless, red-shifted fluorescence band was observed at $\lambda_{max} = 593$ nm. This new band may be caused by either (a) fluorescence from another chemical species, such as an excimer,[40,42] or from aggregates, such as a dimer, or (b) inner filter effects due to high concentrations. While aggregates are not an unreasonable assumption due to the intermolecular B···N interactions observed in the solid state for dimers of **3** (Figure 3d), the estimated molecular sizes of **1** and **3** determined using pulsed field gradient spin−echo (PGSE) NMR measurements[43] indicated the presence of only monomers in solutions.[44] Fluorescence lifetime measurements performed on a range of concentrations of **1** afforded a monoexponential decay consistent with a single-component system with an average lifetime of $\tau = 5.0 \pm 0.3$ ns, effectively ruling out the possibility of an excimer. Thus, this red-shifted band is likely due to an inner filter effect, in which the fluorophore itself absorbs part of the emitted light. This re-absorption causes a reduction of emission intensity and a red-shifted emission band, both of which were

(40) (a) Berlman, I. B. *Handbook of Fluorescence Spectra of Aromatic Molecules*; Academic Press: New York, 1971. (b) Becker, R. S. *Theory and Interpretation of Fluorescence and Phosphorescence*; Wiley-Interscience: New York, 1969. (c) Sharma, A.; Schulman, S. G. *Introduction to Fluorescence Spectroscopy*; Wiley-Interscience: New York, 1999.
(41) (a) Schmidt, W. *J. Chem. Phys.* **1977**, *66*, 828. (b) Dias, J. R. *Handbook of Polycyclic Hydrocarbons Part A: Benzenoid Hydrocarbons*; Elsevier: Amsterdam, 1987.
(42) Forster, T. *Angew. Chem., Int. Ed. Engl.* **1969**, *8*, 333.
(43) (a) Pregosin, P. S.; Kumar, P. G. A.; Fernandez, I. *Chem. Rev.* **2005**, *105*, 2977. (b) Valentini, M.; Pregosin, P. S.; Ruegger, H. *Organometallics* **2000**, *19*, 2551.
(44) The hydrodynamic radii (r_H) for **1** and **3** as determined by PGSE methods were found to be 4.37 and 5.98 Å, respectively, using the following equation: $r_H = [kT/6\pi\eta D]$ (1.11), where η is the viscosity, D is the diffusion coefficient, and 1.11 is a correction factor for elliptical molecules. See: Reger, D. L.; Elgin, J. D.; Semeniuc, R. F.; Pellechia, P. J.; Smith, M. D. *Chem. Commun.* **2005**, 4068. The r_H values for monomers of **1** and **3** as determined by X-ray were found to be 4.52 and 5.66 Å, respectively. These values are more in agreement than those calculated for the dimers, which have X-ray radii values of 6.22 and 7.45 Å, respectively.

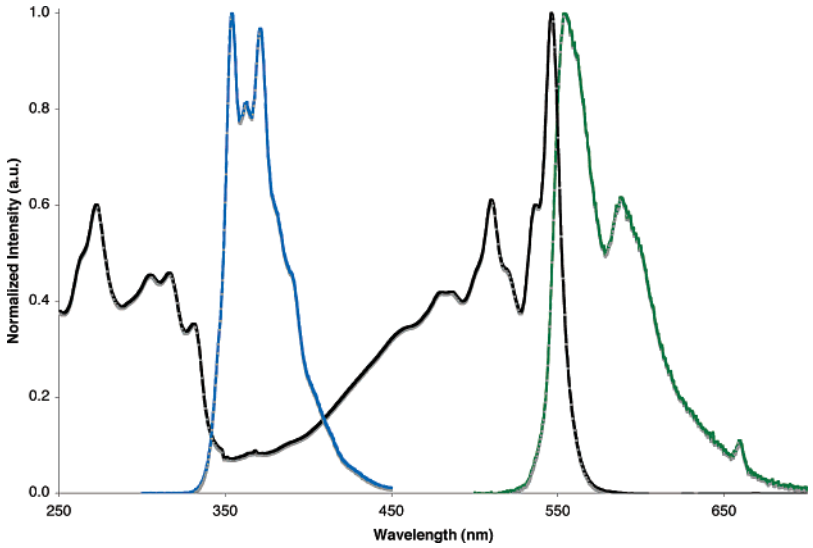

Figure 8. UV−Visible (black) and fluorescence (green) spectra of **1** and fluorescence (blue) spectrum of triphenylene.

Table 3. UV−Visible, Fluorescence, and Quantum Yield Data for **1**−**6**

	UV–Vis[a] (nm) CH_2Cl_2	UV–Vis[a] (nm) hexanes	fluorescence[b] (nm) [color]	Φ_F[c]
1	557 (1.4) 523 (1.0)	546 (1.5) 510 (1.0) 486 (0.7)	558, 586 [yellow−orange]	0.08
2	546 (1.7) 510 (1.3)	537 (0.8) 501 (0.6)	551, 583 [yellow−orange]	0.08
3	545 (2.0) 509 (1.6)	536 (1.3) 500 (1.0)	554, 586 [yellow−orange]	0.08
4	471 (1.5) 447(1.7)	466(1.9) 441 (2.3)	521 [green]	0.02
5	501 (1.8)	493 (3.7)	*d*	
6	622 (0.3) 512 (0.3) 419 (0.3)	605 (0.2) 499 (0.3) 419 (0.3)	*d*	
triphenylene			355, 363, 372 [blue]	0.07[e]

[a] Only the bands in the visible region are reported. Number in parentheses is the extinction coefficient, ϵ (10^4 L mol^{-1} cm^{-1}). [b] Recorded in cyclohexane with excitation at 260 nm. [c] Quantum yield reported relative to 9,10-diphenylanthracene ($\Phi_F = 0.90$). [d] No fluorescence observed. [e] Reference 46b.

observed at high concentration. The quantum yields of **1**−**3** in cyclohexane relative to that of 9,10-diphenylanthracene were all determined to be $\Phi_F = 0.08$, which are indicative of weakly fluorescent species. Small Stokes shift values of 12 nm (**1**), 14 nm (**2**), and 18 nm (**3**) were observed between the absorption and emission spectra, which indicates minimal geometric distortion of the rigid, planar core in the excited state. In comparison, triphenylene has been observed to possess weak blue fluorescence ($\lambda_{max} = 372$ nm), a low quantum yield of $\Phi_F = 0.07$,[45] and conflicting reports on the presence of excimer emission at high concentrations.[46]

Excitation of **4** at 260 nm was found to result in green fluorescence (Figure 7b), with a single broad emission peak centered at 521 nm and a low quantum yield of $\Phi_F = 0.02$. A larger Stokes shift of 55 nm was observed for **4**, which may suggest more pronounced distortion of the larger, and potentially more flexible, planar core in the excited state. The large blue shift in the emission maximum from that of **1**−**3** is also in accordance with the observed blue shift in the absorption spectra. In contrast to **1**−**4**, no fluorescence was observed for **5** and **6**. This is likely due to a nonplanar, twisted geometry caused by steric repulsion of the 3,3′-hydrogen atoms of the diborabiphenyl moiety and the opposing 3,3′-hydrogen atoms of the benzo[*c*]-cinnoline moiety in **5**, or the *ortho* hydrogen atoms of the phenyl groups in **6**, which serves to reduce the aromaticity of the molecules.

Conclusions

The growing role of PAHs as chromophores and conductors in materials chemistry engenders interest in new methods for derivatizing them with a view toward perturbing and tuning their photophysical and/or redox properties.[1] One way to accomplish this is via selective "doping" of PAH frameworks with isoelectronic BN pairs, but this is a significant challenge from a synthetic chemistry point of view. As part of a general program aimed at discovering facile routes to B_nN_n PAH analogues, we have reported here heteroaromatic triphenylene analogues containing $B_2N_2C_2$ cores and explored their structural, redox, and photophysical properties in relation to their all-carbon analogues. The incorporation of boron and nitrogen heteroatoms into the central ring was found to have a dramatic effect on these properties. For example, lower energy charge-transfer absorptions for **1** were found to result in fluorescence in the visible region ($\lambda_{max} = 558$ nm; yellow−orange) with a comparable quantum yield ($\Phi_F = 8\%$) to that of triphenylene, which is weakly fluorescent in the UV/blue region ($\lambda_{max} = 372$ nm, $\Phi_F = 7\%$). As there are numerous examples in the patent literature[47] that utilize PAHs, such as triphenylene, as high efficiency, electroluminescent species in organic-based devices, such as OLEDs and OFETs, the incorporation of this unique class of inorganic/organic hybrid materials might provide an alternative method for color tuning of the active fluorescent

(45) Li, R.; Lim, E. C. *J. Chem. Phys.* **1972**, *57*, 605.
(46) (a) Birks, J. B.; Christophorou, L. G. *Nature* **1962**, *194*, 442. (b) Sasson, R.; Braitbart, O.; Weinreb, A. *J. Lumin.* **1988**, *39*, 223.

(47) See, for example: (a) Inoue, M.; Ukon, M.; Watanabe, T.; Shimizu, Y.; Monobe, H. U.S. Patent 6733849, 2004. (b) Okada, S.; Mizutani, H.; Tsuboyama, A.; Takiguchi, T.; Moriyama, T. U.S. Patent 6528940, 2003. (c) Ishiskawa, H.; Toguchi, S.; Oda, A. U.S. Patent 6492041, 2002. (d) Takiguchi, T.; Okada, S.; Tsuboyama, A.; Nakamura, S.; Moriyama, T. U.S. Patent 6491847, 2002. (e) Paulus, W.; Haussling, L.; Siemensmeyer, K.; Etzbach, K. H.; Adam, D.; Simmerer, J.; Ringsdorf, H.; Schuhmacher, P.; Haarer, D.; Kumar, S. U.S. Patent 6036883, 2000.

layer. In addition, the short B···N interactions observed in **3** provide advantageous structural reinforcement in conjunction with established π-stacking motifs, which may lead to enhanced rigidity, closer molecular contacts, and better overall electron transport properties.

Experimental Section

General Procedures. All reactions and product manipulations were performed under an atmosphere of purified argon using vacuum line techniques or in an M-Braun glovebox using dried solvents. See the Supporting Information for further details.

Synthesis of 1: A solution of pyridazine (0.042 g, 0.52 mmol) in CH_2Cl_2 (5 mL) was slowly added dropwise to a mixture of **H-DBB** and **4,4′-B** (ca. 0.179 g, ca. 0.490 mmol) in CH_2Cl_2 (10 mL) at 25 °C. After 16 h, the volatiles were removed, and the residue was extracted with CH_2Cl_2 (3 × 10 mL) and filtered through Celite. The solvent was removed, and the resulting solid was loaded onto a short column (3 cm) of neutral alumina. The column was washed through with hexanes (15 mL), followed by elution of **1** with CH_2Cl_2. Removal of the solvent gave a black−red solid, which could be further purified by sublimation at 80 °C. X-ray quality crystals of **1** were obtained via slow evaporation of a CH_2Cl_2 solution at 25 °C. Yield: 0.028 g (ca. 41% based on 60:40 ratio of **H-DBB**/**4,4′-B**).

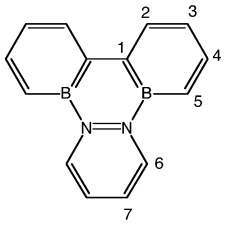

^{1}H NMR ($CDCl_3$): δ = 8.91 (dd, J_{HH} = 3, 6 Hz, H-6), 8.57 (d, J_{HH} = 8 Hz, H-2), 7.85 (dd, J_{HH} = 6, 12 Hz, H-4), 7.61 (d, J_{HH} = 12 Hz, H-5), 7.37 (dd, J_{HH} = 6, 8 Hz, H-3), 6.35 (dd, J_{HH} = 3, 6 Hz, H-7). ^{11}B{^{1}H} NMR ($CDCl_3$): δ = 24.5 (br s). ^{13}C{^{1}H} NMR ($CDCl_3$): δ = ca. 140 (br s, C-5), 139.5 (s, C-4), 134.3 (s, C-6), 128.4 (s, C-3), 125.4 (s, C-2), 110.0 (s, C-7), C-1 was not observed. UV−Vis (ϵ (10^4 L mol^{-1} cm^{-1})): λ_{max} (CH_2Cl_2) = 557 (1.4), 523 (1.0), 321 (0.2), 271 (0.6), 240 (0.7) nm; λ_{max} (hexanes) = 546 (1.5), 510 (1.0), 486 (0.7), 272 (0.6), 221 (0.9) nm. Fluorescence (cyclohexane): λ_{max} = 558, 586 nm, Φ_F = 0.08. Fluorescence lifetime (1.31×10^{-4} M, cyclohexane): τ = 5.0 ns (χ^2 = 3.6). HR-MS for $C_{14}H_{12}N_2{}^{11}B_2$ (M^+): found 230.11795, calcd 230.11866. Cyclic voltammetry (vs SCE): $E_{1/2}$ (THF) = −1.85 (rev), −1.16 (rev), +0.56 (irrev) V; $E_{1/2}$ (CH_2Cl_2) = −2.14 (irrev), −1.35 (rev), +0.60 (irrev) V. Anal. Calcd for $C_{14}H_{12}N_2B_2$ (229.88): C, 73.15; H, 5.26; N, 12.19. Found: C, 72.05; H, 5.48; N, 11.58.

Synthesis of 2: A solution of pyridazine (0.069 g, 0.86 mmol) in toluene (3 mL) was added dropwise over 5 min to a solution of **Me-DBB** (0.343 g, 0.87 mmol) in toluene (10 mL) at 25 °C. After stirring for 24 h, the volatiles were removed, and the resulting solid was washed with cold 2,2,4-trimethylpentane (−78 °C) and dried in vacuo. The solid was then loaded onto a short column of neutral alumina, flushed through with hexanes, and finally eluted with CH_2Cl_2. Removal of the volatiles provided **2** as a dark red solid. Yield: 0.116 g (52%). ^{1}H NMR ($CDCl_3$): δ = 8.71 (dd, J_{HH} = 3, 6 Hz, H-6), 8.31 (s, H-2), 7.68 (d, J_{HH} = 12 Hz, H-4), 7.47 (d, J_{HH} = 12 Hz, H-5), 6.17 (dd, J_{HH} = 3, 6 Hz, H-7), 2.58 (s, C*H*$_3$). ^{11}B{^{1}H} NMR ($CDCl_3$): δ = 24.0 (br s). ^{13}C{^{1}H} NMR ($CDCl_3$): δ = 142.5 (s, C-3), 137.6 (s, C-4), 133.8 (s, C-6), 127.6 (br s, C-5), 123.9 (s, C-2), 108.9 (s, C-7), 24.1 (s, *C*H$_3$), C-1 was not observed. UV−Vis (ϵ (10^4 L mol^{-1} cm^{-1})): λ_{max} (CH_2Cl_2) = 546 (1.7), 510 (1.3), 340 (0.8), 326 (0.9), 275 (1.0), 223 (1.0) nm; λ_{max} (hexanes) = 537 (0.8), 501 (0.6), 334 (0.4), 319 (0.5), 276 (0.6) nm. Fluorescence (cyclohexane): λ_{max} = 551, 583 nm, Φ_F = 0.08. HR-MS for $C_{16}H_{16}N_2{}^{11}B_2$ (M^+): found 258.15145, calcd 258.14996. Cyclic voltammetry (vs SCE): $E_{1/2}$ (THF) = −1.89 (rev), −1.21 (rev), +0.69 (irrev) V; $E_{1/2}$ (CH_2Cl_2) = −1.25 (rev), +0.76 (irrev) V. Anal. Calcd for $C_{16}H_{16}N_2B_2$ (257.93): C, 74.50; H, 6.25; N, 10.86. Found: C, 72.85; H, 7.42; N, 9.28.

Synthesis of 3: A solution of pyridazine (0.057 g, 0.71 mmol) in toluene (3 mL) was added dropwise over 5 min to a solution of the **^{i}Pr-DBB** (0.313 g, 0.695 mmol) in toluene (10 mL) at 25 °C. After stirring for 3 days, the volatiles were removed, and the residue was dissolved in CH_2Cl_2 (25 mL) and filtered to remove any insoluble material. The solvent was removed, and the solid was extracted with 2,2,4-trimethylpentane (15 mL). Removal of the solvent followed by recrystallization from hexanes at −35 °C afforded **3** as X-ray quality dark red−black crystals. An analytically pure sample of **3** was obtained by passing a CH_2Cl_2 solution through a short column of neutral alumina. Yield: 0.129 g (59%). ^{1}H NMR ($CDCl_3$): δ = 8.74 (dd, J_{HH} = 3, 6 Hz, H-6), 8.36 (s, H-2), 7.79 (dd, J_{HH} = 1, 12 Hz, H-4), 7.53 (d, J_{HH} = 12 Hz, H-5), 6.19 (dd, J_{HH} = 3, 6 Hz, H-7), 3.14 (septet, J_{HH} = 7 Hz, ^{i}Pr−C*H*), 1.41 (d, J_{HH} = 7 Hz, ^{i}Pr−C*H*$_3$). ^{11}B{^{1}H} NMR ($CDCl_3$): δ = 24.3 (br s). ^{13}C{^{1}H} NMR ($CDCl_3$): δ = 148.1 (s, C-3), 140.5 (s, C-4), 133.8 (s, C-6), 127.9 (br s, C-5), 121.0 (s, C-2), 108.9 (s, C-7), 36.2 (s, ^{i}Pr-*C*H), 23.9 (s, ^{i}Pr-*C*H$_3$), C-1 was not observed. UV−Vis (ϵ (10^4 L mol^{-1} cm^{-1})): λ_{max} (CH_2Cl_2) = 545 (2.0), 509 (1.6), 323 (1.6), 275 (2.0), 228 (2.2) nm; λ_{max} (hexanes) = 536 (1.3), 500 (1.0), 332 (0.6), 317 (0.8), 304 (0.8), 277 (0.9) nm. Fluorescence (cyclohexane): λ_{max} = 554, 586 nm, Φ_F = 0.08. HR-MS for $C_{20}H_{24}N_2{}^{11}B_2$ (M^+): found 314.21343, calcd 314.21256. Cyclic voltammetry (vs SCE): $E_{1/2}$ (THF) = −1.85 (rev), −1.24 (rev), +0.65 (irrev) V; $E_{1/2}$ (CH_2Cl_2) = −2.02 (irrev), −1.28 (rev), +0.81 (irrev) V. Anal. Calcd for $C_{20}H_{24}N_2B_2$ (314.04): C, 76.49; H, 7.70; N, 8.92. Found: C, 75.27; H, 7.58; N, 8.68. TGA: T_{onset} = 150 °C, $T_{5\%}$ = 208 °C.

Synthesis of 4: A solution of phthalazine (0.091 g, 0.70 mmol) in toluene (3 mL) was added dropwise over 5 min to a solution of **^{i}Pr-DBB** (0.313 g, 0.695 mmol) in toluene (10 mL) at 25 °C. After stirring for 3 days, the volatiles were removed, and the residue was dissolved in CH_2Cl_2 (25 mL) and filtered to remove any insoluble material. The solvent was removed, and the solid was washed with 2,2,4-trimethylpentane (15 mL) and hexanes (15 mL) and dried in vacuo overnight at 25 °C to afford **4** as an orange−brown solid. An analytically pure sample of **4** was obtained by passing a CH_2Cl_2 solution through a short column of neutral alumina. Yield: 0.230 g (91%).

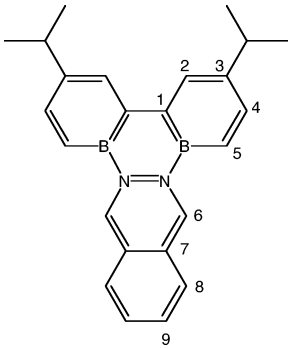

^{1}H NMR ($CDCl_3$): δ = 7.98 (s, H-2), 7.72 (d, J_{HH} = 12 Hz, H-4), 7.51 (d, J_{HH} = 12 Hz, H-5), 7.10 (s, H-6), 7.01 (dd, J_{HH} = 3, 5 Hz, H-8), 6.72 (dd, J_{HH} = 3, 5 Hz, H-9), 3.01 (septet, J_{HH} = 7 Hz, ^{i}Pr−C*H*), 1.35 (d, J_{HH} = 7 Hz, ^{i}Pr−C*H*$_3$). ^{11}B{^{1}H} NMR ($CDCl_3$): δ = 24.1 (br s). ^{13}C{^{1}H} NMR ($CDCl_3$): δ = 148.3 (s, C-3), 141.6 (s, C-4), 134.6 (s, C-7), 129.3 (br s, C-5), 127.8 (s, C-9), 126.2 (s, C-8), 120.8 (s, C-2), 66.8 (s, C-6), 36.1 (s, ^{i}Pr-*C*H), 23.6 (s, ^{i}Pr-*C*H$_3$), 23.4 (s, ^{i}Pr-*C*H$_3$), C-1 was not observed. UV−Vis (ϵ (10^4 L mol^{-1} cm^{-1})): λ_{max} (CH_2Cl_2) = 471 (1.5), 447 (1.7), 291 (1.4), 228 (1.3) nm; λ_{max} (hexanes) = 466 (1.9), 441 (2.3), 288 (1.9), 213 (2.9) nm. Fluorescence (cyclohexane): λ_{max} = 521 nm, Φ_F = 0.02. HR-MS for $C_{24}H_{26}N_2{}^{11}B_2$

(M^+): found 364.22634, calcd 364.22821. Cyclic voltammetry (vs SCE): $E_{1/2}$ (THF) = −1.32 (rev) V; $E_{1/2}$ (CH_2Cl_2) = −1.34 (rev), +1.16 (irrev) V. Anal. Calcd for $C_{24}H_{26}N_2B_2$ (364.10): C, 79.17; H, 7.20; N, 7.69. Found: C, 75.96; H, 6.96; N, 7.23. TGA: T_{onset} = 140 °C, $T_{5\%}$ = 171 °C.

Synthesis of 5: Compound **5** was prepared according to literature procedure.[21a] An analytically pure sample of **5** was obtained by passing a CH_2Cl_2 solution through a short column of neutral alumina. X-ray quality crystals were obtained by slow evaporation of a hexanes/Et_2O (10:1) solution at 25 °C.

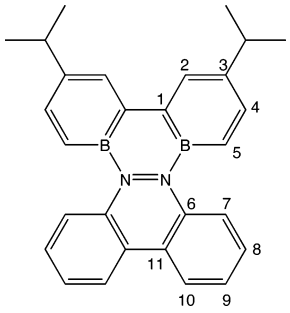

^{1}H NMR ($CDCl_3$): δ = 8.08 (s, H-2), 8.08 (m, H-4), 7.66 (d, J_{HH} = 12 Hz, H-5), 7.47 (m, H-7 + H-10), 7.35 (m, H-8 + H-9), 3.05 (septet, J_{HH} = 7 Hz, ^{i}Pr−C*H*), 1.38 (d, J_{HH} = 7 Hz, ^{i}Pr−CH_3). ^{11}B-{^{1}H} NMR ($CDCl_3$): δ = 27.6 (br s). ^{13}C{^{1}H} NMR ($CDCl_3$): δ = 149.7 (s, C-3), 142.5 (s, C-4), 140.8 (s, C-6), 133.0 (br s, C-5), 128.8 (s, C-9), 128.3 (s, C-7), 125.8 (s, C-8), 123.6 (s, C-11), 122.8 (s, C-10), 121.2 (s, C-2), 36.2 (s, ^{i}Pr-*C*H), 23.3 (s, ^{i}Pr-*C*H_3), C-1 was not observed. UV−Vis (ϵ (10^4 L mol^{-1} cm^{-1})): λ_{max} (CH_2Cl_2) = 501 (1.8), 288 (2.3), 244 (3.1) nm; λ_{max} (hexanes) = 493 (3.7), 285 (4.4), 255 (5.0) nm. Fluorescence (cyclohexane): no fluorescence observed. HR-MS for $C_{28}H_{28}N_2{}^{11}B_2$ (M^+): found 414.24455, calcd 414.24386. Cyclic voltammetry (vs SCE): $E_{1/2}$ (THF) = −1.45 (rev), −1.03 (rev) V; $E_{1/2}$ (CH_2Cl_2) = −1.44 (rev), −1.01 (rev), +1.32 (irrev) V. Anal. Calcd for $C_{28}H_{28}N_2B_2$ (414.16): C, 81.20; H, 6.81; N, 6.76. Found: C, 80.70; H, 7.34; N, 6.17. TGA: T_{onset} = 128 °C, $T_{5\%}$ = 160 °C.

Synthesis of 6: A suspension of diphenylpyridazine (0.161 g, 0.693 mmol) in CH_2Cl_2 (10 mL) was added to a solution of **^{i}Pr-DBB** (0.313 g, 0.695 mmol) in CH_2Cl_2 (15 mL) at 25 °C. After stirring for 3 days, the volatiles were removed, and the residue was extracted with hexanes and filtered. Removal of the solvent afforded **6** as a black solid. An analytically pure sample of **6** was obtained by recrystallization from hexanes at −35 °C. Yield: 0.263 g (81%).

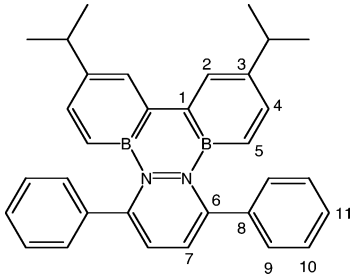

^{1}H NMR ($CDCl_3$): δ = 8.00 (s, H-2), 7.30−7.23 (m, H-9 + H-10 + H-11), 7.14 (dd, J_{HH} = 1, 12 Hz, H-4), 6.52 (d, J_{HH} = 12 Hz, H-5), 6.23 (s, H-7), 2.94 (septet, J_{HH} = 7 Hz, ^{i}Pr−C*H*), 1.30 (d, J_{HH} = 7 Hz, ^{i}Pr−CH_3). ^{11}B{^{1}H} NMR ($CDCl_3$): δ = 27.7 (br s). ^{13}C{^{1}H} NMR ($CDCl_3$): δ = 148.7 (s, C-3), 147.1 (br s, C-1), 146.3 (s, C-6), 142.5 (s, C-8), 139.1 (s, C-4), 133.5 (br s, C-5), 129.0 (s, C-11), 128.9 (s, C-9/C-10), 127.6 (s, C-9/C-10), 120.4 (s, C-2), 112.2 (s, C-7), 36.0 (s, ^{i}Pr−*C*H), 23.4 (s, ^{i}Pr−*C*H_3). UV−Vis (ϵ (10^4 L mol^{-1} cm^{-1})): λ_{max} (CH_2Cl_2) = 622 (0.3), 512 (0.3), 419 (0.3), 248 (0.4) nm; λ_{max} (hexanes) = 605 (0.2), 499 (0.3), 419 (0.3), 223 (0.4) nm. Fluorescence (cyclohexane): no fluorescence observed. HR-MS for $C_{32}H_{32}N_2{}^{11}B_2$ (M^+): found 466.27495, calcd 466.27516. Cyclic voltammetry (vs SCE): $E_{1/2}$ (THF) = −1.68 (rev), −1.20 (rev) V; $E_{1/2}$ (CH_2Cl_2) = −1.80 (irrev), −1.21 (rev), +0.78 (irrev) V. Anal. Calcd for $C_{32}H_{32}N_2B_2$ (466.23): C, 82.44; H, 6.92; N, 6.01. Found: C, 82.10; H, 7.24; N, 5.75. TGA: T_{onset} = 140 °C, $T_{5\%}$ = 250 °C.

Synthesis of [3]$^{\bullet-}$[Cp*$_2$Co]$^+$: A solution of Cp*$_2$Co (0.010 g, 0.03 mmol) in Et_2O (5 mL) was added to a solution of **3** (0.010 g, 0.03 mmol) in Et_2O (5 mL) at 25 °C, which resulted in the immediate formation of a precipitate. After stirring for 24 h, the solid was filtered off, washed with Et_2O (2 mL), and dried in vacuo to afford a dark purple powder of [**3**]$^{\bullet-}$[Cp*$_2$Co]$^+$. X-ray quality crystals were obtained from a THF/Et_2O solution (10:1) at −35 °C. Yield: 0.015 g (75%). ^{1}H NMR (THF-d_8): δ = 2.72 (br s, Cp*-CH_3). UV−Vis (ϵ (10^4 L mol^{-1} cm^{-1})): λ_{max} (THF) = 555 (0.5), 518 (0.5), 490 (0.4), 291 (0.5), 215 (1.4) nm. Fluorescence (THF): λ_{max} = 542, 568, 607 nm. EPR (THF, 25 °C): g_{iso} = 2.002.

Synthesis of [5]$^{\bullet-}$[Cp*$_2$Co]$^+$: A solution of Cp*$_2$Co (0.005 g, 0.02 mmol) in Et_2O (2 mL) was added to a solution of **3** (0.007 g, 0.02 mmol) in Et_2O (5 mL) at 25 °C, which resulted in the immediate formation of a precipitate. After stirring for 24 h, the solid was filtered off, washed with Et_2O (2 mL), and dried in vacuo to afford a dark purple powder of [**5**]$^{\bullet-}$[Cp*$_2$Co]$^+$. Yield: 0.010 g (83%). ^{1}H NMR (THF-d_8): δ = 3.01 (br s, Cp*-CH_3). UV−Vis (ϵ (10^4 L mol^{-1} cm^{-1})): λ_{max} (THF) = 557 (0.5), 440 (0.3), 385 (0.3), 227 (0.3) nm. EPR (THF, 25 °C): g_{iso} = 2.003.

Synthesis of [3]$^{2-}$[Li$^+$(12-crown-4)]$_2$: To a small vial containing a lithium mirror (0.002 g, 0.3 mmol) and 12-crown-4 (0.014 g, 0.079 mmol) was added a solution of **3** (0.007 g, 0.02 mmol) in THF-d_8 (1.5 mL) at 25 °C. After 3 days, the ^{1}H NMR spectrum of the purple solution displayed only broad resonances, suggesting the formation of the radical anion [**3**]$^{\bullet-}$[Li$^+$(12-crown-4)]. ^{1}H NMR (THF-d_8): δ = 3.55 (br s, 12-crown-4). ^{7}Li{^{1}H} NMR (THF-d_8): δ = −0.5 (s, Li$^+$). After a further 3 days, a ca. 2:1 mixture of [**3**]$^{2-}$[Li$^+$(12-crown-4)]$_2$ and [**3**-H]$^-$[Li$^+$-(12-crown-4)] was obtained as a dark red solution.

[3]$^{2-}$[Li$^+$(12-crown-4)]$_2$. ^{1}H NMR (273 K, THF-d_8): δ = 6.35 (s, H-2′), 6.29 (d, J_{HH} = 9 Hz, H-5′), 6.27 (s, H-2″), 6.14 (d, J_{HH} = 8 Hz, H-6′), 5.90 (d, J_{HH} = 11 Hz, H-5″), 5.75 (d, J_{HH} = 9 Hz, H-6″), 4.99 (d, J_{HH} = 9 Hz, H-4′), 4.52 (pseudo t, J_{HH} = 8 Hz, H-7′), 4.21 (dd, J_{HH} = 11, 1 Hz, H-4″), 4.13 (pseudo t, J_{HH} = 9 Hz, H-7″), 3.55 (s, 12-c-4), 2.61 (septet, J_{HH} = 7 Hz, ^{i}Pr−C*H*), 2.23 (septet, J_{HH} = 7 Hz, ^{i}Pr−C*H*), 1.17 (d, J_{HH} = 7 Hz, ^{i}Pr−CH_3), 1.02 (d, J_{HH} = 7 Hz, ^{i}Pr−CH_3). ^{7}Li{^{1}H} NMR (273 K, THF-d_8): δ = 0.5 (s, Li$^+$). ^{11}B{^{1}H} NMR (273 K, THF-d_8): δ = 28.2 (br s).

[3-H]$^-$[Li$^+$(12-crown-4)]. ^{1}H NMR (273 K, THF-d_8): δ = 7.44 (d, J_{HH} = 2 Hz, H-5′), 7.29 (d, J_{HH} = 2 Hz, H-5″), 6.61 (dd, J_{HH} = 10, 2 Hz, H-4′), 6.53 (dd, J_{HH} = 10, 2 Hz, H-4″), 6.52 (t, J_{HH} = 3 Hz, H-6/7), 5.99 (d, J_{HH} = 10 Hz, H-2′), 5.56 (t, J_{HH} = 3 Hz, H-6/7), 5.19 (d, J_{HH} = 10 Hz, H-2″), 4.66 (t, J_{HH} = 3 Hz, H-6/7), 3.55 (s, 12-c-4), 2.66 (septet, J_{HH} = 7 Hz, ^{i}Pr−C*H*), 2.62 (septet, J_{HH} = 7 Hz, ^{i}Pr−C*H*), 1.18 (d, J_{HH} = 7 Hz, ^{i}Pr−CH_3), 1.14 (d, J_{HH} = 7 Hz, ^{i}Pr−CH_3). ^{7}Li-{^{1}H} NMR (273 K, THF-d_8): δ = −0.9 (s, Li$^+$). ^{11}B{^{1}H} NMR (273 K, THF-d_8): δ = 28.2 (br s).

Acknowledgment. This work was funded by the Natural Sciences and Engineering Research Council (NSERC) of Canada in the form of a Discovery Grant to W.E.P. The Alberta Ingenuity Fund is thanked for providing postdoctoral fellowship support to C.A.J. (2005−2007) and D.J.H.E. (2002−2003) and a studentship to M.J.D.B, and NSERC of Canada is acknowledged for a postdoctoral fellowship to C.A.J. (2005−2007) and a PGS-D scholarship to M.J.D.B. The authors would also like to thank Dorothy Fox for help with the PGSE experiments, Brett Chandler for help with obtaining the TGA data, Heikki Tuononen for performing the SOMO calculations on [**1**]$^{\bullet-}$, Carol

Ladner for help with running the fluorescence lifetime experiments, and Prof. Dan Nocera (MIT), Prof. David Cramb (Calgary), and Prof. Ray Turner (Calgary) for helpful discussions regarding the fluorescence experiments and/or for use of their equipment.

Supporting Information Available: General experimental procedures and protocols for precursor synthesis and product characterization, table of selected bond lengths and torsion angles for all structures, table of calculated NICS values for **1** and triphenylene, HOMO, LUMO, and SOMO orbital pictures, cyclic voltammogram of **1**, EPR spectra for $[\mathbf{3}]^{\bullet-}$ and $[\mathbf{5}]^{\bullet-}$ (14 pages, print/PDF). Crystallographic data for **1**, **3**, **5**, and $[\mathbf{3}]^{\bullet-}[Cp^*_2Co]^+$ in CIF format. This material is available free of charge via the Internet at http://pubs.acs.org.

JA063519P